Spin-Lattice Coefficients for Gd^{3+} and Eu^{2+} in CaF_2 and for Gd^{3+} in CaO†

R. CALVO* AND R. A. ISAACSON
University of California, San Diego, La Jolla, California 92037

AND

Z. SROUBEK‡
University of California, Los Angeles, California 90007

(Received 26 August 1968)

We have measured the spin-lattice coefficients of Eu^{2+} and Gd^{3+} in CaF_2 and Gd^{3+} in CaO by studying the effect of uniaxial stress on the EPR spectra of these ions. The experimental data show that fourth-order terms in the spin-lattice Hamiltonian give significant contributions. The values of the second-order spin-lattice coefficients are given, and the fourth-order contribution is tentatively identified as due to the change of the cubic field splitting with stress. From the value of the fourth-order coefficient, we conclude that at least half of the temperature dependence of the cubic field parameter is due to the effect of the lattice expansion.

I. INTRODUCTION

IN his classical papers Van Vleck[1,2] assumed that the interaction which produces the relaxation in magnetically dilute paramagnetic ions in crystals is purely electric and comes from the modulation of the crystalline electric field at the position of the impurity due to the thermal vibrations of the lattice. This idea has been successful in explaining the experimental data on relaxation times. In these calculations it is necessary to estimate the interaction between the paramagnetic ion and the electric field gradients produced by the deformation of the lattice. The strength of this interaction is given by the so-called spin-lattice coefficients. The knowledge of these coefficients enables one not only to predict spin-lattice relaxation times but also contributes to the understanding of the nature of the interaction between the ion and the lattice.[3]

The first experiments[4,5] to measure directly the value of the spin-lattice coefficients were done by two different experimental methods. One is the measurement of the shift of the energy levels in a crystal under uniaxial stress by observing the shifts of the EPR (electron paramagnetic resonance) lines.[4,6] The other uses ultrasonic techniques and gives the values of the coefficients from measurements of the interaction of phonons with the paramagnetic ion.[5,7]

In the present work we study the behavior of rare-earth S-state ions in a cubic environment under deformations of the lattice, using the uniaxial-stress method. Previous work on these ions is discussed in Sec. V. We report measurements on Eu^{2+} and Gd^{3+} in the CaF_2 lattice and of Gd^{3+} in CaO. The paramagnetic ions are in an eightfold coordination of fluorines in CaF_2 and in a sixfold coordination of oxygens in CaO.

In order to explain the experimental data, we use a formalism similar to that used by Feher[6] for Mn^{2+} and Fe^{3+} in MgO. A brief account of our preliminary values was published[8] in this notation. However, in our case the data do not fit a theory where only second-order terms are considered. It is necessary, therefore, to include fourth-order terms in the spin-lattice Hamiltonian to explain the data.

We define spin-lattice coefficients which, in second order, are equivalent to C_{11} and C_{44} as defined in Ref. 6. These correspond, respectively, to tetragonal and trigonal deformations in the second-order Hamiltonian. There are also three fourth-order coefficients corresponding to the three deformations: completely symmetrical, tetragonal, and trigonal.

Our experimental data allow us to find the values of the second-order coefficients. One of the fourth-order coefficients gives an important contribution to the shifts and is tentatively identified as the coefficient corresponding to the completely symmetrical deformation. The value of this coefficient is used to explain the temperature dependence of the cubic field splitting by assuming that this dependence is due to the thermal expansion of the lattice.

In Sec. II we give the formalism of the interaction up to fourth-order terms in the Hamiltonian. Section III gives the values of the shifts as a function of the stress coefficients for the cases of experimental importance and we discuss the difference on the behavior of second- and fourth-order terms. Section IV deals with the experimental data and gives the values of the spin-lattice coefficients. A discussion of the experimental errors is included. In Sec. V we discuss our values for

† Work supported by the National Science Foundation.

* Fellow of the Consejo Nacional de Investigaciones Científicas y Técnicas de la República Argentina. Present address: Centro Atomico Bariloche, San Carlos de Bariloche (R. N.) Republica Argentina.

‡ On leave from the Institute of Radio Engineering and Electronics, Czechoslovak Academy of Science, Prague, Czechoslovakia.

[1] J. H. Van Vleck, J. Chem. Phys. **7**, 72 (1939).
[2] J. H. Van Vleck, Phys. Rev. **72**, 426 (1940).
[3] M. Blume and R. Orbach, Phys. Rev. **127**, 1587 (1962).
[4] G. D. Watkins and E. Feher, Bull. Am. Phys. Soc. **7**, 29 (1962).
[5] N. Shiren, Bull. Am. Phys. Soc. **7**, 29 (1962).
[6] Elsa Rosenvasser Feher, Phys. Rev. **136**, A135 (1964).
[7] See, for example, E. B. Tucker, Proc. IEEE **53**, 1547 (1965).
[8] R. Calvo and Z. Sroubek, Bull. Am. Phys. Soc. **13**, 901 (1968).

the second- and fourth-order stress coefficients. The temperature dependence of the cubic field splitting is also discussed.

II. FORMULATION OF THE PROBLEM

The EPR spectrum of a rare-earth S-state impurity ion in a slightly deformed cubic crystal is described by the spin Hamiltonian

$$H=g\beta\mathbf{H}_0\cdot\mathbf{S}+H_{\text{cub}}+H',$$

where $g\beta\mathbf{H}_0\cdot\mathbf{S}$ is the usual Zeeman energy term. H_{cub} has a form

$$H_{\text{cub}}=B_4(O_4^0+5O_4^4)+B_6(O_6^0-21O_6^4), \quad (1)$$

where the O_n^m are the Stevens equivalent spin operators[9] and B_4 and B_6 are phenomenological parameters. H' is a small perturbation produced by the deformation of the crystal and can be written in terms of the spin operators $O_{\Gamma_i}^{\alpha(n)}$ given in the Appendix as

$$H'=\sum_{n,i,\alpha} G_{\Gamma_i}^{(n)}O_{\Gamma_i}^{\alpha(n)}Q_{\Gamma_i}^{\alpha}, \quad (2)$$

where $Q_{\Gamma_i}^{\alpha}$ are the normal deformations of the lattice which transform like the α component of the Γ_i representation and are tabulated in the Appendix. $G_{\Gamma_i}^{(n)}$ is the corresponding spin-lattice coefficient. It is the purpose of this work to find the values of these coefficients.

It is helpful to choose the Q's to be the normal coordinates of the system of nearest ligands in units of the lattice parameter. In CaF_2 eight fluorines surround the impurity; of the 24 coordinates of this cube, only nine are important in our problem; the others represent odd symmetry modes. These nine modes transform like $\Gamma_{1g}+\Gamma_{3g}+2\Gamma_{5g}$ in the cubic group and are given by Leushin[10] and Huang and Inoue.[11] In addition, only six of these modes can be changed by an external uniform stress. Six coordinates must be considered for H' in the CaF_2 lattice and they transform like $\Gamma_{1g}+\Gamma_{3g}+\Gamma_{5g}$. In the CaO lattice, the normal modes of the octahedron of oxygen also transform like $\Gamma_{1g}+\Gamma_{3g}+\Gamma_{5g}$ in the cubic group. Hence, the same modes contribute in both cases.

The perturbation Hamiltonian H for rare-earth ions contain second-, fourth-, and sixth-order spin operators. Our experimental data can be described using second- and fourth-order terms only. Then for our experiments where $Q_{\Gamma_{3g}^{\upsilon}}=Q_{\Gamma_{5g}^{\xi}}=Q_{\Gamma_{5g}^{\eta}}=0$, the Hamiltonian H can be written as follows:

$$\begin{aligned}H'=&G_{\Gamma_{1g}}^{(4)}(O_4^0+5O_4^4)Q_{\Gamma_{1g}}\\&+[G_{\Gamma_{3g}}^{(2)}O_2^0+G_{\Gamma_{3g}}^{(4)}(O_4^0-7O_4^4)]Q_{\Gamma_{3g}^{u}}\\&+[G_{\Gamma_{5g}}^{(2)}O_2^2(s)+G_{\Gamma_{5g}}^{(4)}O_4^2(s)]Q_{\Gamma_{5g}^{\zeta}}. \quad (3)\end{aligned}$$

[9] M. T. Hutchings, in *Solid State Physics*, edited by F. Seitz and D. Turnbull (Academic Press Inc., New York, 1964), Vol. 16.

[10] A. M. Leushin, Fiz. Tverd. Tela **5**, 605 (1963) [English transl.: Soviet Phys.—Solid State **5**, 440 (1963)].

[11] C. Y. Huang and M. Inoue, J. Phys. Chem. Solids **25**, 889 (1964).

The normal deformations of the lattice, $Q_{\Gamma_i}^{\alpha}$, are expressed in terms of linear combinations of the components of the strain tensor, as shown in the Appendix. This transformation can be found in the literature but we have changed some numerical factors in order to be consistent with previous nomenclature in uniaxial-stress experiments. If we assume that the local compression equals the bulk value, the strain is related to the external stress by the relation

$$\epsilon_{ij}=\sum_{k,l} s_{ijkl}X_{kl},$$

where X_{kl} are the components of the stress tensor and s_{ijkl} are the elastic constants of the crystal.

The perturbation given by H' is usually much smaller than the Zeeman energy contribution to the levels. Also, as a consequence of the microwave frequency used in these experiments, the Zeeman energy is much larger than the contribution of the cubic field H_{cub}. The wave functions of the system can be approximated by S_z eigenstates, where z is the coordinate axis along the direction of the magnetic field. The perturbation H' must be transformed to this system and the shifts of the EPR lines can be easily found from its diagonal matrix elements.

III. EVALUATION OF THE SPIN-LATTICE COEFFICIENTS FOR OUR EXPERIMENTAL CASES

Equation (3) gives the value of the interaction for a given deformation. In order to clarify the procedure we used for the analysis of the experimental data, we will specialize Eq. (3) to the cases of interest. The transformation rules of the Stevens' operators tabulated by Hutchings[9] are used in these calculations.

$\mathbf{P}$ denotes the external stress and $\mathbf{H}_0$ denotes the external magnetic field.

Case A: $P\|[001]$, $H_0\|[100]$

The components of the stress tensor are $X_{33}=P$, $X_{11}=X_{22}=X_{12}=X_{13}=X_{23}=0$; then the components of the strain tensor are

$$\epsilon_{11}=\epsilon_{22}=s_{12}P, \quad \epsilon_{33}=s_{11}P, \quad \epsilon_{12}=\epsilon_{13}=\epsilon_{23}=0.$$

Using the definitions given in the Appendix for the amplitude of the normal modes in terms of the strain tensor,

$$\begin{aligned}&Q_{\Gamma_{1g}}=(s_{11}+2s_{12})P,\\&Q_{\Gamma_{3g}^{u}}=(s_{11}-s_{12})P/2, \quad \text{and all others are zero.}\end{aligned} \quad (4)$$

Then H', referred to the cubic axis, is given by

$$\begin{aligned}H'=&G_{\Gamma_{1g}}^{(4)}(O_4^0+5O_4^4)(s_{11}+2s_{12})P\\&+[G_{\Gamma_{3g}}^{(2)}O_2^0+G_{\Gamma_{3g}}^{(4)}(O_4^0-7O_4^4)](s_{11}-s_{12})P/2. \quad (5)\end{aligned}$$

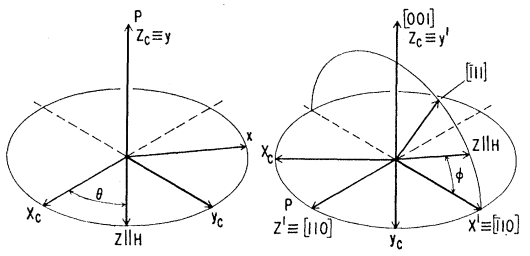

FIG. 1. (a) Case $\mathbf{P} \parallel [001]$ and $\mathbf{H} \perp [001]$. (b) Case $\mathbf{P} \parallel [110]$ and $\mathbf{H} \perp [\bar{1}10]$. In both cases, x_c, y_c, and z_c are the cubic axes and x, y, and z the axes where the perturbation introduced by the stress is calculated.

Experimentally, it is more convenient to measure the external stress P rather than the deformation, so spin-lattice coefficients related to stress rather than strain are used. The stress coefficients, $C_{\Gamma_i}^{(n)}$, are related to the strain coefficients, $G_{\Gamma_i}^{(n)}$, by

$$C_{\Gamma_{1g}}^{(n)} = G_{\Gamma_{1g}}^{(n)}(s_{11}+2s_{12}), \tag{6a}$$

$$C_{\Gamma_{3g}}^{(n)} = G_{\Gamma_{3g}}^{(n)}(s_{11}-s_{12}), \tag{6b}$$

$$C_{\Gamma_{5g}}^{(n)} = G_{\Gamma_{5g}}^{(n)} s_{44}. \tag{6c}$$

Then, Eq. (5) can be written as

$$H' = C_{\Gamma_{1g}}^{(4)} P(O_4^0 + 5O_4^4) + C_{\Gamma_{3g}}^{(2)}(\tfrac{1}{2}P)O_2^0 + C_{\Gamma_{3g}}^{(4)}(\tfrac{1}{2}P)(O4^0 - 7O_4^4). \tag{7}$$

This Hamiltonian is referred to the crystalline axes. We want to transform it to a system where the z axis is in the (001) plane (and therefore perpendicular to the direction of the stress) and parallel to the direction of the magnetic field [see Fig. 1(a)].

In this system the diagonal part of the Hamiltonian is given as a function of θ by

$$H' = C_{\Gamma_{1g}}^{(4)} P(\tfrac{3}{8} + \tfrac{5}{8}\cos 4\theta)O_4^0 - \tfrac{1}{4}C_{\Gamma_{3g}}^{(2)} P O_2^0 + C_{\Gamma_{3g}}^{(4)} P(\tfrac{3}{16} - \tfrac{7}{16}\cos 4\theta)O_4^0. \tag{8}$$

For $\mathbf{H}_0 \parallel [100]$,

$$H' = C_{\Gamma_{1g}}^{(4)} P O_4^0 - \tfrac{1}{4}C_{\Gamma_{3g}}^{(2)} P O_2^0 - \tfrac{1}{4}C_{\Gamma_{3g}}^{(4)} P O_4^0, \tag{9}$$

and the shifts in energy ΔE and in magnetic field ΔH for the fine-structure lines are

$$\Delta E_{3/2\leftrightarrow 1/2} = 720 C_{\Gamma_{1g}}^{(4)} P - \tfrac{3}{2}C_{\Gamma_{3g}}^{(2)} P + 180 C_{\Gamma_{3g}}^{(4)} P = -g\beta\Delta H_{3/2\leftrightarrow 1/2}, \tag{9a}$$

$$\Delta E_{5/2\leftrightarrow 3/2} = 600 C_{\Gamma_{1g}}^{(4)} P - 3C_{\Gamma_{3g}}^{(2)} P + 150 C_{\Gamma_{3g}}^{(4)} P = -g\beta\Delta H_{5/2\leftrightarrow 3/2}, \tag{9b}$$

$$\Delta E_{7/2\leftrightarrow 5/2} = -1200 C_{\Gamma_{1g}}^{(4)} P - \tfrac{9}{2}C_{\Gamma_{3g}}^{(2)} P - 300 C_{\Gamma_{3g}}^{(4)} P = -g\beta\Delta H_{7/2\leftrightarrow 5/2}, \tag{9c}$$

with $\Delta E_{M_S\leftrightarrow M_S-1} = \Delta E_{-M_S\leftrightarrow -M_S+1}$. The contribution of the second-order terms to the shifts are identical to those obtained in Ref. 6. Note that our respective coefficients are related, so $C_{\Gamma_{3g}}^{(2)} = C_{11}$ and $C_{\Gamma_{5g}}^{(2)} = C_{44}$. The fourth-order contributions are angle-dependent in this plane, as shown in Eq. (8).

Case B: $P[110]$, $H_0 \perp [110]$

The components of the stress tensor are in this case

$$X_{11} = X_{22} = X_{12} = P/2, \quad X_{13} = X_{23} = X_{33} = 0.$$

Then, for the strain tensor we have

$$\epsilon_{11} = \epsilon_{22} = \tfrac{1}{2}P(s_{11}+s_{12}), \qquad \epsilon_{33} = Ps_{12},$$
$$\epsilon_{12} = \tfrac{1}{2}Ps_{44}, \qquad \epsilon_{13} = \epsilon_{23} = 0,$$

and the values of the displacements of the normal coordinates are

$$\begin{aligned} &Q_{\Gamma_{1g}} = (s_{11}+2s_{12})P, \\ &Q_{\Gamma_{3g}{}^u} = -\tfrac{1}{4}(s_{11}-s_{12})P, \\ &Q_{\Gamma_{5g}{}^\xi} = \tfrac{1}{2}s_{44}P, \quad \text{and all others are zero.} \end{aligned} \tag{10}$$

The Hamiltonian (3) is in this case

$$H' = C_{\Gamma_{1g}}^{(4)} P(O_4^0 + 5O_4^4) - \tfrac{1}{4}C_{\Gamma_{3g}}^{(2)} P O_2^0 - \tfrac{1}{4}C_{\Gamma_{3g}}^{(4)} P(O_4^0 - 7O_4^4) + \tfrac{1}{2}C_{\Gamma_{5g}}^{(2)} P O_2^2(s) + \tfrac{1}{2}C_{\Gamma_{5g}}^{(4)} P O_4^2(s), \tag{11}$$

where we have used (6a), (6b), (6c), and (10).

In order to transform Eq. (11) to a coordinate system where the z axis is in the direction of the magnetic field, we perform two successive rotations of the system. First, we refer it to a coordinate system where z' is along the [110] direction [see Fig. 1(b)] and then to the final xyz system. In $x'y'z'$, we have

$$\begin{aligned} H' = {} & C_{\Gamma_{1g}}^{(4)} P(-\tfrac{1}{4}O_4^0 + 5O_4^2 + (15/4)O_4^4) \\ & + C_{\Gamma_{3g}}^{(2)} P(\tfrac{1}{8}O_2^0 + \tfrac{3}{8}O_2^2) \\ & + C_{\Gamma_{3g}}^{(4)} P(-\tfrac{5}{16}O_4^0 + \tfrac{1}{4}O_4^2 - (21/16)O_4^4) \\ & + C_{\Gamma_{5g}}^{(2)} P(\tfrac{1}{4}O_2^0 - \tfrac{1}{4}O_2^2) \\ & + C_{\Gamma_{5g}}^{(4)} P(-\tfrac{1}{16}O_4^0 - \tfrac{1}{4}O_4^2 + \tfrac{7}{16}O_4^4). \end{aligned}$$

In the system xyz, the diagonal part of the Hamiltonian H' as a function of the angle φ is

$$\begin{aligned} H' = {} & C_{\Gamma_{1g}}^{(4)} P(-\tfrac{3}{32} - \tfrac{5}{8}\cos 2\varphi + \tfrac{15}{32}\cos 4\varphi) \\ & + C_{\Gamma_{3g}}^{(2)} P(-\tfrac{1}{16} + \tfrac{3}{16}\cos 2\varphi)O_2^0 + C_{\Gamma_{3g}}^{(4)} P(-(15/128) - \tfrac{1}{32}\cos 2\varphi - (21/128)\cos 4\varphi)O_4^0 \\ & + C_{\Gamma_{5g}}^{(2)} P(-\tfrac{1}{8} - \tfrac{1}{8}\cos 2\varphi)O_2^0 + C_{\Gamma_{5g}}^{(4)} P(-(3/128) + \tfrac{1}{32}\cos 2\varphi + (7/128)\cos 4\varphi)O_4^0, \end{aligned} \tag{12}$$

where $\mathbf{H}_0 \parallel [001]$ corresponds to $\varphi = 90°$, $\mathbf{H}_0 \parallel [111]$ to $\varphi = 35°\,15'$, and $H_0 \parallel [\bar{1}10]$ to $\varphi = 0°$.

For $\mathbf{H}_0 \parallel [001]$, the Hamiltonian (12) is

$$H' = C_{\Gamma_{1g}}^{(4)} P O_4^0 - \tfrac{1}{4}C_{\Gamma_{3g}}^{(2)} P O_2^0 - \tfrac{1}{4}C_{\Gamma_{3g}}^{(4)} P O_4^0. \tag{13}$$

TABLE I. Spin-lattice coefficients in units of cm/dyne. The values for Eu^{2+} and Gd^{3+} in CaF_2 were taken at 77°K, and for $CaO:Gd^{3+}$ at 1.4°K. The cubic field-splitting parameters are given in units of 10^{-4} cm^{-1}.

	$CaF_2:Eu^{2+}$	$CaF_2:Gd^{3+}$	$CaO:Gd^{3+}$	Estimated error
$b_4=60B_4$	-57.9 ± 0.2[a]	-48.4 ± 0.3[b]	-12.28 ± 0.01[c]	
$b_6=1260B_6$	$+0.5\pm0.2$[a]	$+0.1\pm0.3$[b]	$+1.18\pm0.01$[c]	
$C_{11}=C_{\Gamma_{3g}}^{(2)}$	-1.71×10^{-13}	-1.80×10^{-13}	$+0.66\times10^{-13}$	10%
$C_{44}=C_{\Gamma_{5g}}^{(2)}$	-10.9×10^{-13}	-3.0×10^{-13}	-5.35×10^{-13}	10%
$C_{\Gamma_{1g}}^{(4)}-\frac{1}{4}C_{\Gamma_{3g}}^{(4)}$	$+0.10\times10^{-15}$	$+0.10\times10^{-15}$	$+0.10\times10^{-15}$	25%
$C_{\Gamma_{1g}}^{(4)}+\frac{3}{16}C_{\Gamma_{5g}}^{(4)}$	$>+0.08\times10^{-15}$ $<+0.20\times10^{-15}$	$>+0.0\times10^{-15}$ $<+0.15\times10^{-15}$		
$C_{\Gamma_{1g}}^{(4)}-\frac{1}{4}-(5C_{\Gamma_{3g}}^{(4)}+C_{\Gamma_{5g}}^{(4)})$			$>+0.0\times10^{-15}$ $<+0.5\times10^{-15}$	

[a] From Ref. 14. [b] From Ref. 14. [c] Our results.

This formula is identical to Eq. (9), and so the shifts of the fine-structure lines for this case are given by Eqs. (9a), (9b), and (9c).
For $\mathbf{H}_0 \parallel [\bar{1}11]$ it is

$$H'=-\tfrac{2}{3}C_{\Gamma_{1g}}^{(4)}PO_4^0-\tfrac{1}{6}C_{\Gamma_{5g}}^{(2)}PO_2^0-\tfrac{1}{8}C_{\Gamma_{5g}}^{(4)}PO_4^0, \quad (14)$$

and for $\mathbf{H}_0 \parallel [\bar{1}10]$ we have

$$H'=-\tfrac{1}{4}C_{\Gamma_{1g}}^{(4)}PO_4^0-\tfrac{1}{4}(-\tfrac{1}{2}C_{\Gamma_{3g}}^{(2)}+C_{\Gamma_{5g}}^{(2)})PO_2^0 +\tfrac{1}{16}(-5C_{11}^{(4)}+C_{11}^{(4)})PO_4^0. \quad (15)$$

When we consider the matrix elements of O_2^0 and O_4^0 in (8) and (12) we see the principal difference between the second- and fourth-order contributions. Second-order contributions shift the fine-structure lines $\pm\frac{7}{2}\leftrightarrow\pm\frac{5}{2}$, $\pm\frac{5}{2}\leftrightarrow\pm\frac{3}{2}$, and $\pm\frac{3}{2}\leftrightarrow\pm\frac{1}{2}$ in the ratio 3:2:1, while the fourth-order contribution produces shifts of the same lines in the ratio 10:−5:−6. This fact allows one to verify the presence of fourth-order contributions by measuring the ratio of the shifts of the different fine-structure lines of the EPR spectra in almost any direction of stress and magnetic field (the exceptions are some singular directions where the angularly-dependent part is zero).

However, from Eqs. (8), (13), (14), and (15) we see that it is not easy to separate the different fourth-order contributions unless a complete study of the variation of the shifts with the direction of $\mathbf{H}_0$ is performed. Unfortunately, because Eu^{2+} and Gd^{3+} have very anisotropic spectra in a cubic environment, a small change in the orientation of the sample when the stress is applied produces shifts of the positions of the EPR lines. The magnitude of these shifts is comparable with the change due to the fourth-order terms of the interaction and has the same dependence on the fine-structure lines [the cubic field splitting is due mainly to fourth-order terms in the spin Hamiltonian, as seen in Eq. (1)]. These spurious fourth-order contributions are negligible when the magnetic field is in the direction of the cubic axes.

IV. EXPERIMENTAL RESULTS

The experiments were performed with two different EPR spectrometers with facilities to apply uniaxial stress to the sample. One is at 9 GHz and was described in Ref. 6 and the other at 35 GHz and was described in Ref. 12. The crystals used in these experiments were obtained from Semi Elements, Inc. In the case of the CaF_2 samples, the concentrations of the paramagnetic fluoride were about 0.05%. In the case of the CaO samples, Gd^{3+} was an unintentional impurity and its concentration is less than 0.01%. The data were taken at 300°K for Eu^{2+} in CaF_2, 77°K for Gd^{3+} in CaF_2, and 1.3°K for Gd^{3+} in CaO.

The EPR spectra of Eu^{2+} and Gd^{3+} in a cubic environment have been studied by different authors,[13–15] and the experimental values for the constants of the spin Hamiltonian Eq. (1) are tabulated in Table I.

We observed linewidths of 5 to 15 G for the different fine-structure transitions of Eu^{2+} and Gd^{3+} in CaF_2. In the case of Gd^{3+} in CaO the linewidths are 0.1 G for the central transition and less than 2 G for the other transitions when the magnetic field H_0 is parallel to the cubic axis. The linewidths of $CaO:Gd^{3+}$ reflect the internal stresses of the sample. In the case of Gd^{3+} and Eu^{2+} in CaF_2 the predominant factor is the unresolved superhyperfine structure with the fluorines.

The samples were stressed along the [001] and [110] directions up to about 600 kg/cm². The most useful data were found in a sample stressed in the [110] direction and with the magnetic field $\mathbf{H}_0$ parallel to the [001], [$\bar{1}$11], and [$\bar{1}$10] directions. For each orientation of the magnetic field the shift of the fine-structure lines was measured as a function of stress. In the case of $\mathbf{H}_0 \parallel [\bar{1}10]$, the spectra of Gd^{3+} and Eu^{2+} in CaF_2 is not well resolved and so only a pair of transitions could be measured. In the case of Gd^{3+} in CaO it was not possible to measure the shifts for $\mathbf{H}_0 \parallel [\bar{1}11]$ because the EPR lines overlap lines from other impurities. We found in every case that the central fine-structure transition ($M_S=-\frac{1}{2}\leftrightarrow\frac{1}{2}$) is not affected by the stress. This

[12] Z. Sroubek, M. Tachiki, P. H. Zimmermann, and R. Orbach, Phys. Rev. **165**, 435 (1968).
[13] R. Lacroix, Helv. Phys. Acta **30**, 374 (1957).
[14] C. Ryter, Helv. Phys. Acta **30**, 395 (1957).
[15] Alexander J. Shuskus, Phys. Rev. **127**, 2022 (1962).

justifies Eq. (3) where only even powers of spin are allowed in H'.

It was observed that the shifts of the fine-structure transitions do not follow the ratio 3:2:1 for the $\frac{7}{2}\leftrightarrow\frac{5}{2}$, $\frac{5}{2}\leftrightarrow\frac{3}{2}$, $\frac{3}{2}\leftrightarrow\frac{1}{2}$ lines, as expected if only second-order contributions in (3) are important. The data were fitted with Eqs. (9), (13), (14), and (15), where contributions up to fourth order are considered. We have found the values of the second- and fourth-order spin-lattice coefficients from the shifts of two of the three nonconjugate fine-structure transitions (conjugate transitions like $\pm M_S\leftrightarrow\pm M_S\pm 1$ give the same shift but in opposite directions). The value of the shift of the third transition with stress serves as a cross check.

Because of the anisotropy of the EPR spectra of Eu^{2+} and Gd^{3+} (in a cubic environment) with the direction of the magnetic field $\mathbf{H}_0$, small changes in the orientation of the sample when the stress is applied produce significant shifts of the lines. Only when $\mathbf{H}_0$ is parallel to the cubic axis is the change of the positions of the lines negligible for small changes in the position of the sample in an arbitrary direction. The cubic field splitting is mainly due to fourth-order terms in the spin Hamiltonian (1). Hence, when the orientation of $\mathbf{H}_0$ is slightly altered, the positions of the transitions $\frac{7}{2}\leftrightarrow\frac{5}{2}$, $\frac{5}{2}\leftrightarrow\frac{3}{2}$, and $\frac{3}{2}\leftrightarrow\frac{1}{2}$ change in the ratio $10:-5:-6$. This is a major source for the determination of fourth-order coefficients in directions of the magnetic field other than $\mathbf{H}_0\parallel[100]$. In order to make an estimation of the magnitude of this effect we calculate for Eu^{2+} and Gd^{3+} in CaF_2 a shift of the fine-structure transition $\frac{7}{2}\leftrightarrow\frac{5}{2}$ of about 5 G when the direction of the magnetic field changes only $\frac{1}{2}$ deg in the plane perpendicular to its plane of rotation and for $\mathbf{H}_0\parallel[\bar{1}11]$. This shift is larger than that observed for the fourth-order contribution for $\mathbf{H}_0\parallel[001]$ (see Fig. 1). For this reason, it was impossible to perform a measurement of the angular variation of the fourth-order contribution to the shift

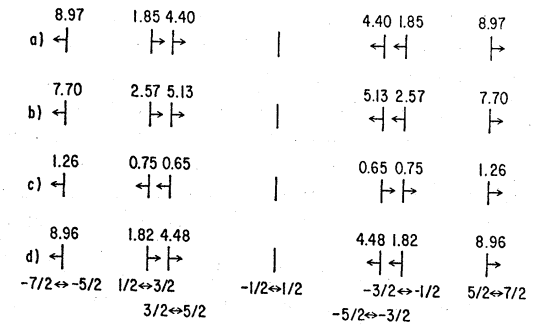

FIG. 2. Shifts of the EPR lines of $CaF_2:Eu^{2+}$ for $\mathbf{P}\parallel[110]$ and $\mathbf{H}\parallel[001]$ corresponding to $P=1$ dyne/cm^2; (a) experimental shifts, (b) second-order contribution to the shift as calculated with $C_{\Gamma_{3g}}{}^{(2)}=-1.71\times10^{-13}$ cm/dyne, (c) fourth-order contribution to the shift as calculated with $(C_{\Gamma_{1g}}{}^{(4)}-\frac{1}{4}C_{\Gamma_{3g}}{}^{(4)})=+0.1\times10^{-15}$ cm/dyne, (d) total shift as predicted including second- and fourth-order contributions. The shifts are given in 10^{-13} cm^{-1} per dyne/cm^2 (or 10^{-13} cm/dyne).

to separate the contributions from completely symmetrical, tetragonal, and trigonal fourth-order spin-lattice coefficients. However, our experimental values suggest that the important fourth-order contribution is given by the completely symmetrical deformation as discussed in Sec. VB.

Our experimental values of the spin-lattice coefficients for Eu^{2+} and Gd^{3+} in CaF_2 and for Gd^{3+} in CaO are given in Table I with estimated errors. The signs of the second-order coefficients are defined in the same way as in Ref. 6. In order to clarify this definition and to give an idea of the contribution to the shifts of second- and fourth-order terms in H', we give in Fig. 2 the changes of the positions of the lines as measured in our experiments and compare these with calculated contributions to the shift. They are given in units of cm/dyne (or cm^{-1} per dyne/cm^2).

V. SPIN-LATTICE COEFFICIENTS

A. Second-Order Spin-Lattice Coefficients

First, we compare our values for the second-order stress coefficients to previous work. Dobrov[16] has reported measurements of G_{44} on $CaF_2:Eu^{2+}$ by the ultrasonic technique. His value $|G_{44}|=(0.3\pm0.1)$ cm^{-1} and our value $G_{44}=(-0.38\pm0.04)$ cm^{-1} as obtained from Table I using Eq. (6c) are in good agreement within the experimental errors. This agreement shows the independence of the spin-lattice coefficients on the frequency of the measurement as predicted by Van Vleck.[2] (For uniaxial static stress this frequency is zero compared with 10^{10} Hz for the ultrasonic method.) This agreement was also found between the data for iron group ions by the uniaxial-stress method[4] and the ultrasonic method.[5]

Simultaneously with our preliminary report,[8] data for Eu^{2+} in CaF_2, SrF_2 and BaF_2 by the uniaxial-stress method were reported by Hopson and Nolle.[17] In the case of Eu^{2+} in CaF_2 they found $G_{11}=(-0.22\pm0.05)$ cm^{-1} and $G_{44}=(-0.39\pm0.05)$ cm^{-1} in good agreement with our values: $G_{11}=(-0.20\pm0.02)$ cm^{-1} and $G_{44}=(-0.38\pm0.04)$ cm^{-1}.

Data for C_{11} and C_{44} in Gd^{3+} in CaF_2 has been obtained by the uniaxial-stress method by Bowden and Miller.[18] They obtain $C_{11}=(3.6\pm0.8)10^{-13}$ cm/dyne and $C_{44}=(8.2\pm0.4)10^{-13}$ cm/dyne. We have no explanation for the severe disagreement in magnitude and sign between these values and ours.

There is no available theory for rare-earth ions which would explain our experimental C_{11} and C_{44} in terms of microscopical parameters. Nevertheless, the comparison with available data for similar but obviously more covalent iron group ions (Mn^{2+} and Fe^{3+}) is of some

[16] W. I. Dobrov, Phys. Rev. 134, A734 (1964).
[17] J. W. Hopson and A. W. Nolle, Bull. Am. Phys. Soc. 13, 885 (1968).
[18] C. M. Bowden and J. E. Miller, Bull. Am. Phys. Soc. 13, 245 (1968).

interest. The values of the stress coefficients for iron group ions increase with the valency of the ions as predicted by the covalency model. On the other hand, the stress parameters for the rare-earth ions remain constant or even decrease as the valency of the cations increases. This tendency is consistent with the electrostatic ionic-model approach, as this model predicts C_{11} and C_{44} proportional to the mean value of some power of the ionic radius (e.g., $\langle r^2\rangle$, $\langle r^4\rangle$). The wave functions of ions having lower valency are more spread out, which implies larger values for $\langle r^n\rangle$ and so larger values for C_{11} and C_{44} as obtained for the rare-earth ions.

B. Fourth-Order Spin-Lattice Coefficients

A surprising result is found in Table I. Even if the values of the second-order coefficients differ in magnitude and sign for the different cases, this difference is not present in the value of $C_{\Gamma_{1g}}{}^{(4)}-\frac{1}{4}C_{\Gamma_{3g}}{}^{(4)}$. Also, by looking at the other two rows of Table I, where only upper and lower limits for some linear combinations of the fourth-order coefficients are given, we are tempted to suppose that we are measuring the value of $C_{\Gamma_{1g}}{}^{(4)}$, i.e., it gives rise to the dominant fourth-order contribution to H' in our experiments.

If this is the case, we are then measuring the change with the lattice parameter of the cubic field parameter B_4 defined in Eq. (2). From Eqs. (1) and (3)

$$G_{\Gamma_{1g}}{}^{(4)}=\frac{\Delta B_4}{Q_{\Gamma_{1g}}}=\frac{\Delta B_4}{\epsilon_{11}+\epsilon_{22}+\epsilon_{33}}=\frac{\Delta B_4}{3\Delta a/a},$$

where a is the lattice parameter, Δa is its change due to the completely symmetrical deformation, and ΔB_4 is the change of the cubic parameter B_4. From our values of the stress coefficients and the elastic constants of the crystals,[19] we find, using Eq. (6a),

$$G_{\Gamma_{1g}}{}^{(4)}=(C_{\Gamma_{1g}}{}^{(4)}/s_{11}+2s_{12})=2.6\times10^{-4}\ \text{cm}^{-1}.$$

There are no data available on the effect of hydrostatic pressure on the EPR spectra of Gd^{3+} and Eu^{2+} in crystals to compare with our values. However, there are data for the $3d$ S-state ions Mn^{2+} and Fe^{3+}. Walsh[20] has studied the pressure dependence of the cubic field parameter in MgO up to 10^4 kg/cm^2. For the highest pressure applied, he found a change of the cubic field parameter B_4 of 0.68×10^{-6} cm^{-1} for Mn^{2+} and 7.3×10^{-6} cm^{-1} for Fe^{3+}. In our notation, and using the known elastic constants of MgO,[19] we calculate $Q_{\Gamma_{1g}}=0.64\times10^{-2}$. The values of the fourth-order strain coefficients in these cases are estimated to be

$$G_{\Gamma_{1g}}{}^{(4)}=1.06\times10^{-4}\ \text{cm}^{-1}\quad\text{for } Mn^{2+}\text{ in MgO},$$
$$G_{\Gamma_{1g}}{}^{(4)}=11.4\times10^{-4}\ \text{cm}^{-1}\quad\text{for } Fe^{3+}\text{ in MgO}.$$

These values are suggestive of those we have observed for the f^7 ions. At present, no satisfactory explanation for the cubic field splitting exists and we are unable to estimate how these quantities vary with lattice distortion. It is interesting to see, however, why no fourth-order contributions were observed for Mn^{2+} and Fe^{3+} in MgO in Ref. 6. In view of the size of the coefficients calculated above, the change of B_4 for a hypothetical force of 1 dyne/cm^2 are

$$B_4=0.22\times10^{-16}\ \text{cm}^{-1}\quad\text{for MgO:}Mn^{2+},$$
$$B_4=2.5\times10^{-16}\ \text{cm}^{-1}\quad\text{for MgO:}Fe^{3+},$$
$$B_4=1.0\times10^{-16}\ \text{cm}^{-1}\quad\text{for } Gd^{3+}\text{ and } Eu^{2+}\text{ in } CaF_2.$$

For an external stress of 5×10^8 dynes/cm^2 the shift of the positions of the lines for $\mathbf{H}_0\parallel[100]$ are

MgO:Mn^{2+}, 0.028 G	for the $\frac{5}{2}\leftrightarrow\frac{3}{2}$ transition;
MgO:Fe^{3+}, 0.32 G	for the $\frac{5}{2}\leftrightarrow\frac{3}{2}$ transition;
Eu^{2+} and Gd^{3+} in CaF_2, 1.2 G	for the $\frac{7}{2}\leftrightarrow\frac{5}{2}$ transition.

For the rare-earth ions Eu^{2+} and Gd^{3+}, the shifts of the lines due to second-order contributions in H' are small compared with those obtained for Mn^{2+} and Fe^{3+} in MgO. In fact, $C_{\Gamma_{3g}}{}^{(2)}$ is about five times larger for Mn^{2+} in MgO than for the rare earths in CaF_2 and about 15 times larger for Fe^{3+}. Thus, fourth-order contributions are masked by the strong second-order contribution for the iron group ions.

Another feature closely related to the change of the cubic field parameter with lattice constant is the temperature dependence of the cubic field splitting. If it is assumed that this dependence is due to the effect of the change of the lattice parameter with the thermal expansion of the crystal, we can predict its magnitude using our pressure results. The thermal change of the cubic field splitting G_{TE} is given by

$$G_{\text{TE}}=\Delta B_4/Q_{\Gamma_{1g}}=\Delta B_4/3\alpha\Delta T,$$

where ΔB_4 is the change of the cubic-field parameter in the range of temperature ΔT and α is the linear expansion coefficient of the lattice.

Using the data of Ref. 21 for the temperature change of B_4 and a linear expansion coefficient $\alpha=1.8\times10^{-5}/°\text{K}$ extrapolated from the data in Ref. 22, we find an "experimental" value of

$$G_{\text{TE}}=5.0\times10^{-4}\ \text{cm}^{-1}.$$

[19] H. B. Huntington, in *Solid State Physics*, edited by F. Seitz and D. Turnbull (Academic Press Inc., New York, 1958), Vol. 7, p. 214.
[20] W. M. Walsh Jr., Phys. Rev. **122**, 762 (1961).
[21] T. Rewaj, Fiz. Tverd. Tela **9**, 2978 (1967) [English transl.: Soviet Phys.—Solid State **9**, 2340 (1968)].
[22] D. N. Batchelder and R. O. Simmons, J. Chem. Phys. **41**, 2324 (1964).

This value is about twice the value of $G_{\Gamma_{1g}}{}^{(4)}$ but with the same sign. We conclude from our analysis that at least half of the temperature dependence of the cubic field parameter is due to the effect of the lattice expansion. Other contributions due to dynamical interactions of the ion with phonons have been calculated,[23–25] but it was found that these contributions are not important and they have an incorrect temperature dependence.[25]

ACKNOWLEDGMENTS

We would like to thank Dr. Elsa Feher, Professor R. Orbach, and Professor G. Feher for the use of their spectrometers, and for many comments and suggestions.

[23] Chao Yuan Huang, Phys. Rev. **159**, 683 (1967).
[24] T. J. Menne, J. Phys. Chem. Solids **28**, 1629 (1967).
[25] T. J. Menne, Phys. Rev. **170**, 356 (1968).

APPENDIX A: LINEAR COMBINATIONS OF THE STEVENS OPERATORS WHICH TRANSFORM LIKE IRREDUCIBLE REPRESENTATIONS OF THE CUBIC GROUP

$$O_{\Gamma_{1g}}{}^{(4)}=O_4{}^0+5O_4{}^4;$$
$$O_{\Gamma_{3g}{}^u}{}^{(2)}=O_2{}^0;$$
$$O_{\Gamma_{3g}{}^u}{}^{(4)}=O_4{}^0-7O_4{}^4;$$
$$O_{\Gamma_{5g}{}^\xi}{}^{(2)}=O_2{}^2(s);$$
$$O_{\Gamma_{5g}{}^\xi}{}^{(4)}=O_4{}^2(s).$$

APPENDIX B: DEFINITION OF THE NORMAL COORDINATES IN TERMS OF THE STRAIN TENSOR ϵ_{nm}

$$Q_{\Gamma_{1g}}=(\epsilon_{xx}+\epsilon_{yy}+\epsilon_{zz});$$
$$Q_{\Gamma_{3g}{}^u}=\tfrac{1}{4}(2\epsilon_{zz}-\epsilon_{xx}-\epsilon_{yy});\quad Q_{\Gamma_{3g}{}^v}=\tfrac{3}{4}(\epsilon_{xx}-\epsilon_{yy});$$
$$Q_{\Gamma_{5g}{}^\xi}=\epsilon_{yz};\quad Q_{\Gamma_{5g}{}^\eta}=\epsilon_{xz};\quad Q_{\Gamma_{5g}{}^\zeta}=\epsilon_{xy}.$$

PHYSICAL REVIEW VOLUME 177, NUMBER 2 10 JANUARY 1969

Dynamic Jahn-Teller Effect of MgO:Cu^{++} at 4.2°K

K. ŽĎÁNSKÝ
Institute of Radio Engineering and Electronics, Czechoslovak Academy of Sciences, Prague, Czechoslovakia
(Received 5 April 1968)

The electron-spin-resonance spectrum of Cu^{++} in MgO was observed at 4.2°K. This spectrum is explained in terms of the dynamic Jahn-Teller effect when an adiabatic approach is used. In addition it is compared with the spectrum of Sc^{++} in fluorides for which a nonadiabatic approach is seen to be in agreement with the experimental g values. The difference between these two systems is explained when the lattice polarization is taken into account.

INTRODUCTION

THE theory of Jahn-Teller effect of E_g-state ions in the cubic crystal field has been studied thoroughly.[1–4] It is one of the important features of these previous studies that the usual Born-Oppenheimer approximation is not valid. The total wave function cannot be written as a product of the nuclear and electronic wave functions. This important feature must be taken into account when dynamic effects are expected. In the study by O'Brien[4] it was assumed that the electronic state follows the distortion exactly, since the motion of the nuclei should be slow compared to that of the electrons. Under this assumption, the g values and hyperfine coupling constants were calculated by neglecting the overlap between vibronic functions. In contrast, Bersuker[5] considers the splitting of the threefold degenerate vibronic ground state given by the tunneling effect. However, in his study, though it is not stated explicitly, an approximation other than that used in all previous studies is employed. The vibronic wave functions used by Bersuker are given by a product of the vibrational and electronic wave functions, which may be interpreted as implying that the electronic states do not follow the distortion adiabatically. Nevertheless, quite recently[6] Bersuker's approach was successfully used to explain the experimental g values of Sc^{++} in CaF_2 and SrF_2. In the present study we shall calculate the g values of the vibronic state caused by the tunneling between the three degenerate

[1] J. H. Van Vleck, J. Chem. Phys. **7**, 72 (1939).
[2] U. Öpik and M. H. L. Pryce, Proc. Roy. Soc. (London) **A238**, 425 (1957).
[3] H. C. Longuet-Higgins, U. Öpik, M. H. L. Pryce, and R. A. Sack, Proc. Roy. Soc. (London) **A244**, 1 (1958).
[4] M. C. M. O'Brien, Proc. Roy. Soc. (London) **A281**, 323 (1964).
[5] J. B. Bersuker, Zh. Eksperim. i Teor. Fiz. **43**, 1315 (1962); **44**, 1239 (1963) [English transl.: Soviet Phys.—JETP **16**, 933 (1963); **17**, 836 (1963)].
[6] U. T. Höchli, Phys. Rev. **162**, 262 (1967).